ChemComm

ROYAL SOCIETY OF CHEMISTRY

COMMUNICATION

View Article Online
View Journal

Check for updates

Cite this: DOI: 10.1039/d0cc02767g

Received 16th April 2020,
Accepted 21st July 2020

DOI: 10.1039/d0cc02767g

rsc.li/chemcomm

Accessing new microporous polyspirobifluorenes *via* a C/Si switch†

Andrei Nesmelov, David Lee, Christopher Bejger, Margaret Kocherga,
Zachary Lyles, Madeline K. Greenier, Ashley Ariel Vitallo, Ghallia Kaouk,
Daniel S. Jones and Thomas A. Schmedake *

Microporous spirosilabifluorene networks were synthesized *via* Yamamoto coupling of tetrabromospirosilabifluorene precursors. They exhibit bright fluorescence that is quenched in the presence of nitroaromatics. The C/Si switch has subtle effects on the optical properties of the spirobifluorene network and provides a convenient route to 3,3′,6,6′-coupled and other polybifluorenes.

Condensed microporous networks are receiving considerable attention for gas and energy storage, sensing, and catalysis applications.[1] The 9,9′-spirobifluorene motif, particularly significant for electronic applications,[2,3] has also emerged as a popular structural unit that acts as a contortion site to create materials with intrinsic microporosity.[4–23] Yamamoto coupling of the readily available 2,2′,7,7′-tetrabromo-9,9′-spirobifluorene, with $Ni(COD)_2$ was shown to produce a very high surface area microporous network, and co-polymerization under similar conditions with rigid dibrominated aromatic struts provided materials with tunable optical and gas sorption properties.[24,25] Other methods have also produced homo-polymeric or co-polymeric networks starting from the 2,2′,7,7′-tetrabromo-9,9′-spirobifluorene reagent.

There has been relatively little exploration of condensed networks based on polymerization at the more tetrahedrally directing 3,3′,6,6′ positions of the 9,9′-spirobifluorene, likely a result of the inherent challenge of selectively halogenating at the 3,3′,6,6′ positions. One recent strategy to selectively halogenate at the 3,3′,6,6′ positions involved initial methoxylation at the 2,2′,7,7′ positions then reacting with I_2/PIFA to afford the 2,2′,7,7′-tetramethoxy-3,3′,6,6′-tetraiodo-9,9′-spirobifluorene precursor.[26] Further modification of this precursor has led to nucleobase-decorated tetrapodands.[27] The tetraalkyne was subsequently polymerized *via* Sonogashira and acetelynic coupling reactions to generate a spirobifluorene framework that can act as a support for Pd and Pt catalysed hydrogenation.[28] A direct synthetic route to 3,3′,6,6′-tetrabromospirobifluorene would be attractive for sensing, gas storage, catalysis and other applications but remains elusive.

On the other hand, access to the silicon-centered analog, 3,3′,6,6′-tetrabromospirosilabifluorene, and its derivatives is relatively straightforward *via* modification of the Gilman method,[29] providing a direct route to a tetrahedral-directing structural motif for condensed polymeric networks. However, to what extent will a Si center affect the properties of the condensed spirobifluorene network? Spirosilabifluorenes have been extensively studied recently for optical, electronic, and sensing applications,[30–35] and the C/Si switch typically leads to a lower LUMO due to contribution from the Si-σ* orbitals.[36] In this manuscript, we demonstrate the synthetic versatility of brominated spirosilabifluorenes and explore the microporous networks derived from Yamamoto condensation of the 2,2′,7,7′- and 3,3′,6,6′-tetrabrominated spirosilabifluorenes.

The precursors 2,2′,7,7′-tetrabromo-9,9′-spriosilabifluorene, **1**, and 3,3′6,6′-tetrabromo-9,9′-spriosilabifluorene, **2**, were synthesized *via* cyclization of the appropriate 2,2′-dilithiodibromobiphenyl with silicon tetrachloride (Scheme 1).

Single crystals of compounds **1** and **2** were obtained and their structures determined with X-ray crystallography (Fig. 1). Both possess a similar structural motif with orthogonal dibromofluorene units surrounding a silicon spirocenter. Compound **1** is structurally analogous to the carbon analog 2,2′,7,7′-tetrabromo-9,9′-spirobifluorene, **1-C**, which was also used in this study for comparison. Compound **2** on the other hand provides access to tetrahedral-oriented cross-couplings.

Yamamoto coupling of compounds **1**, **1-C**, and **2** with $Ni(COD)_2$ under anaerobic conditions produced the corresponding polyspirosilabifluorenes, **PS1** and **PS2**, and the previously reported polyspirobifluorene, **PS1-C** as an insoluble, microporous material (Scheme 2). The surface areas of the materials were determined using BET surface area analysis with nitrogen as adsorbate following the criteria for microporous material analysis recommended by IUPAC.[37] The surface area

---

Department of Chemistry, University of North Carolina – Charlotte, Charlotte, NC 28223, USA. E-mail: Tom.Schmedake@uncc.edu

† Electronic supplementary information (ESI) available: NMR spectra, adsorption isotherms, structure data, diffuse reflectance, SEM, IR spectra, and quenching studies. CCDC 1995230 and 1995231. For ESI and crystallographic data in CIF or other electronic format see DOI: 10.1039/d0cc02767g

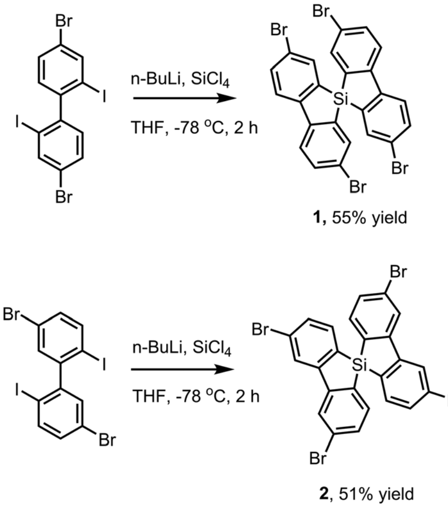

Scheme 1 Synthesis of **1** and **2**. The halogenated precursors were synthesized according to literature procedures.[44,45]

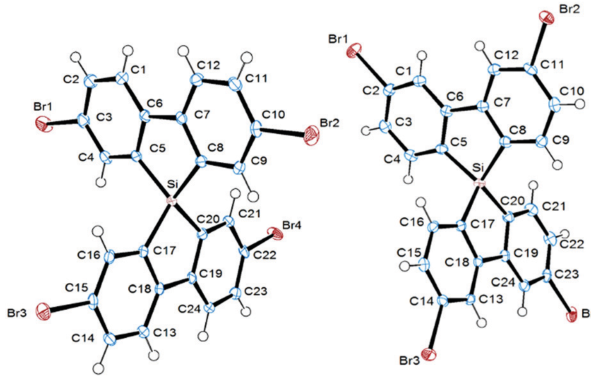

Fig. 1 ORTEP representation of **1** (left, solvent molecule excluded), which crystallized in space group $P\bar{1}$, and **2** (right) in space group *Pbca*.

we obtained for **PS1-C**, 1980 $m^2\ g^{-1}$, is consistent with the previously reported value of 1970 $m^2\ g^{-1}$.[25] It is apparent that the C/Si switch appears to lower the overall surface area for both **PS1** and **PS2**. In addition, the tetrahedral directed 3,6-diyl coupling in **PS2** produces smaller pores and lower overall pore volume, consistent with the ability to form smaller rings (Table 1).

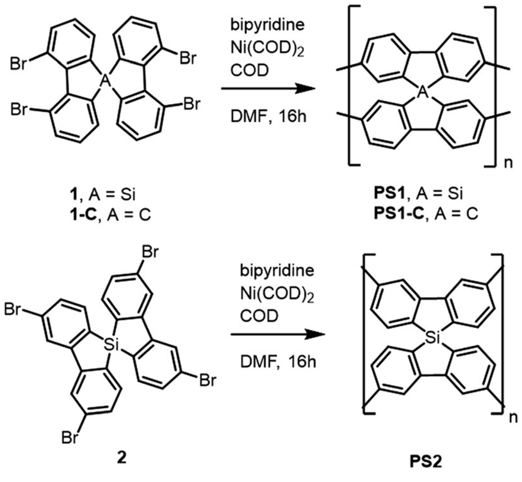

Scheme 2 Synthesis of **PS1**, **PS1-C**, and **PS2**.

Table 1 Results of BET analysis

Sample	SA_{BET} ($m^2\ g^{-1}$)	V_{pore} (DFT)[a] (mL g^{-1})	Pore width[a] (nm)
PS1	1420	1.15	1.7
PS2	1520	0.865	1.5
PS1-C	1980	1.70	1.7

[a] DFT analysis using NLDFT model of N_2 at 77 K on carbon with cylindrical pores (additional info available in ESI).

Each of the samples was suspended in acetonitrile using sonication, and the resulting suspensions were used to obtain the fluorescence excitation and emission spectra (Fig. 2). **PS1** and **PS1-C** were similar in their fluorescence spectra. Both samples possessed a low energy shoulder in the excitation spectrum centered at λ_{ex} = 412 nm for **PS1-C** and λ_{ex} = 406 for **PS1**. Likewise, both samples emitted a broad peak centered around λ_{em} = 464 nm for **PS1-C** and λ_{em} = 454 nm for **PS1**.

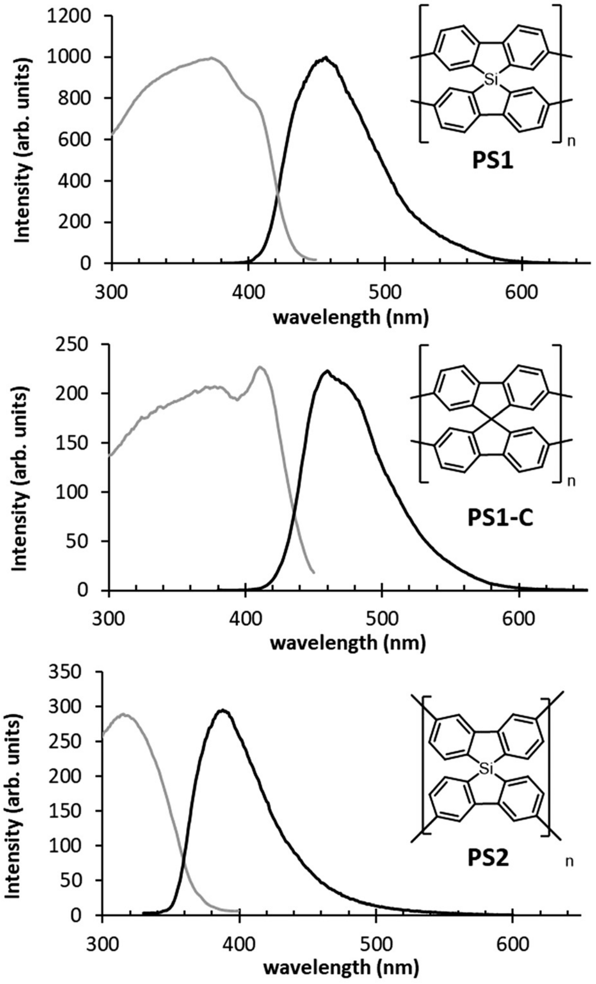

Fig. 2 Excitation (gray) and emission spectra of (top) **PS1**, (middle) **PS1-C**, and (bottom) **PS2**.

PS2 on the other hand was significantly shifted towards higher energy, λ_{ex} = 317 nm and λ_{em} = 389 nm. Tauc plots were obtained from the diffuse reflectance UV-vis (DRUV) spectra to obtain band gaps of 2.9 eV for both **PS1** and **PS1-C** and 3.6 eV for **PS2**.

DFT calculations (B3LYP/6-31G*, gas state) were performed to understand the observed optical properties (Fig. 3). As a model system, we optimized the geometry and performed energy calculations on oligomers of increasing length up to pentamers. For simplicity, we only considered polymerization of one of the fluorene groups. The theoretical results clearly indicate that the positioning of the fluorene coupling (*i.e.* 2,2′,7,7′ *vs.* 3,3′,6,6′) has a greater effect on the $\Delta E_{LUMO-HOMO}$ gap than the identity of the central atom. The difference can already be seen in the HOMO of the optimized dimers in Fig. 3. In the HOMO of the C3-coupled dimer, the C1,C4 and C5,C8 carbon atoms of the fluorene rings are part of nodal surfaces, reducing overall conjugation length in the C3-coupled dimer relative to the HOMO of the C2-coupled dimer. This effect continues with increasing oligomers, leading to a significantly larger $\Delta E_{LUMO-HOMO}$, approximately 0.6 eV higher in energy for the 3,6-coupled spirosilabifluorene pentamer relative to the 2,7-coupled spirosilabifluorene pentamer. This is consistent with the blue shift of 0.7 eV in the band gap of **PS2** relative to **PS1**.

On the other hand, the calculations would predict a much smaller red shift of approximately only 0.1 eV for **PS1** relative to **PS1-C** as a result of the Si-σ* orbital contribution to the LUMO in an idealized structure. However, the difference in band gaps from DRUV spectroscopy and the Tauc plots is negligible. This suggests that the effect of the Si-σ* orbital contribution is subtle compared to other structural factors, such as chain length and torsion angles that are likely constrained in the three-dimensional matrix and significantly affect the optical and electronic properties of polyfluorenes.

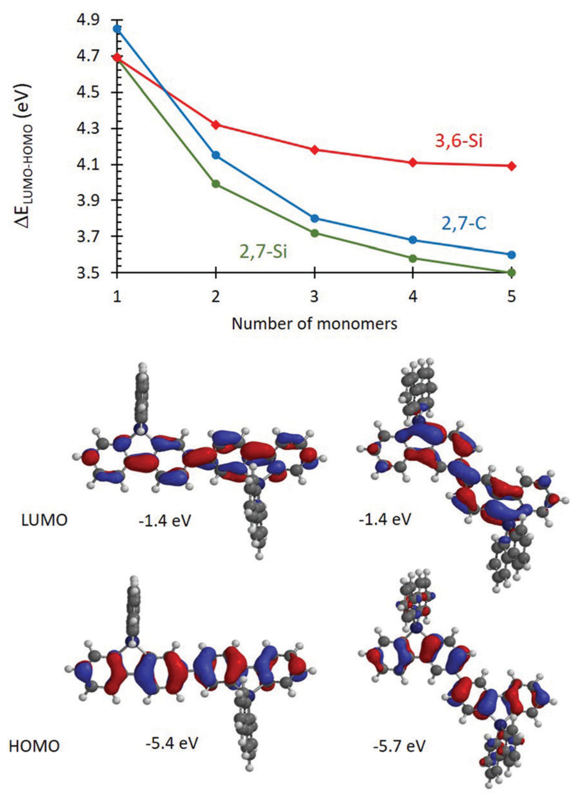

Fig. 3 Theoretical results of DFT calculations. Band gap as a function of monomer repeat units (top). HOMOs and LUMOs of spirosilabifluorene-2,2′-diyl dimer (left) and spirosilabifluorene-3,3′-diyl dimer (right).

Likewise, the effect of the C/Si switch was not apparent in nitroaromatic quenching studies. Stern–Volmer quenching studies were conducted on samples suspended in acetonitrile to determine the sensitivity of the microporous materials towards various nitroaromatic analytes (Table 2). The trend of increasing analyte sensitivity for the series NB < DNT < TNT is consistent with published data for other silafluorene based nitroaromatic sensors.[38–43] However, we are unable to identify any trends with respect to the specific nature of the polyspirobifluorene matrix.

We can conclude that tetrabrominated spirosilabifluorenes provide easy access *via* Yamamoto coupling to luminescent, high surface area, microporous materials and that both polyspirobifluorenes and polysilaspirobifluorenes are potential substrates for fluorescence based sensing of nitroaromatics. The negligible solubility of the highly cross-linked materials could be attractive for specific sensing applications, and the microporous nature could provide enhanced sensitivity for gas phase sensing. Any electronic effects from the C/Si switch are negligible compared to the difference resulting from the position of fluorene-coupling. A significant advantage of the C/Si switch from a synthetic viewpoint, is the relative ease of forming tetrabromospirosilabifluorene. This strategy could be implemented to synthesize a wide range of monomers with modifications and regiospecificities difficult to access with the carbon-centered spirobifluorene. It could also be readily adopted to asymmetrically substituted spirosilabifluorene monomers. Subsequent polymerization of these novel spirosilabifluorene centers could provide a wide range of new homo- and heteropolymeric materials of intrinsic microporosity for electronic, sensing, gas storage, and catalytic applications.

This material is based upon work supported by the National Science Foundation under Grant No. 1800331. We also gratefully acknowledge Dr Juan Vivero-Escoto for the use of the Surface Area Analyzer. Additional financial support from the UNC Charlotte Department of Chemistry and the Thomas Walsh Tuition Fellowship are also appreciated.

Table 2 Results of Stern–Volmer quenching experiments

Analyte	Sample	K_{sv} (L mol^{-1})
Nitrobenzene	**PS1**	530
NB	**PS2**	338
	PS1-C	452
2,6-Dinitrotoluene	**PS1**	861
DNT	**PS2**	1130
	PS1-C	861
2,4,6-Trinitrotoluene	**PS1**	1190
TNT	**PS2**	1600
	PS1-C	2370

Conflicts of interest

There are no conflicts to declare.

Notes and references

1 For recent reviews see: (*a*) Y. F. He, X. D. Zhuang, C. J. Lei, L. C. Lei, Y. Hou, Y. Y. Mai and X. L. Feng, *Nano Today*, 2019, **24**, 103–119; (*b*) R. B. Lin, S. C. Xiang, H. B. Xing, W. Zhou and B. L. Chen, *Coord. Chem. Rev.*, 2019, **378**, 87–103; (*c*) P. Sudarsanam, E. Peeters, E. V. Makshina, V. I. Parvulescu and B. F. Sels, *Chem. Soc. Rev.*, 2019, **48**, 2366–2421; (*d*) H. Wang, Z. T. Zeng, P. Xu, L. S. Li, G. M. Zeng, R. Xiao, Z. Y. Tang, D. L. Huang, L. Tang, C. Lai, D. N. Jiang, Y. Liu, H. Yi, L. Qin, S. J. Ye, X. Y. Ren and W. W. Tang, *Chem. Soc. Rev.*, 2019, **48**, 488–516; (*e*) K. Wang, D. D. Qi, Y. L. Li, T. Y. Wang, H. B. Liu and J. Z. Jiang, *Coord. Chem. Rev.*, 2019, **378**, 188–206; (*f*) J. L. Wu, F. Xu, S. M. Li, P. W. Ma, X. C. Zhang, Q. H. Liu, R. W. Fu and D. C. Wu, *Adv. Mater.*, 2019, **31**, 1802922; (*g*) Y. Zheng, S. S. Zheng, H. G. Xue and H. Pang, *J. Mater. Chem. A*, 2019, **7**, 3469–3491.

2 M. Saliba, S. Orlandi, T. Matsui, S. Aghazada, M. Cavazzini, J. P. Correa-Baena, P. Gao, R. Scopelliti, E. Mosconi, K. H. Dahmen, F. De Angelis, A. Abate, A. Hagfeldt, G. Pozzi, M. Graetzel and M. K. Nazeeruddin, *Nat. Energy*, 2016, **1**, 15017.

3 T. P. I. Saragi, T. Spehr, A. Siebert, T. Fuhrmann-Lieker and J. Salbeck, *Chem. Rev.*, 2007, **107**, 1011–1065.

4 J. Weber, O. Su, M. Antonietti and A. Thomas, *Macromol. Rapid Commun.*, 2007, **28**, 1871–1876.

5 J. Weber, M. Antonietti and A. Thomas, *Macromolecules*, 2008, **41**, 2880–2885.

6 J. Weber and A. Thomas, *J. Am. Chem. Soc.*, 2008, **130**, 6334–6335.

7 S. W. Yuan, S. Kirklin, B. Dorney, D. J. Liu and L. P. Yu, *Macromolecules*, 2009, **42**, 1554–1559.

8 J. Weber, J. Schmidt, A. Thomas and W. Bohlmann, *Langmuir*, 2010, **26**, 15650–15656.

9 J. Weber, *ChemSusChem*, 2010, **3**, 181–187.

10 J. Brandt, J. Schmidt, A. Thomas, J. D. Epping and J. Weber, *Polym. Chem.*, 2011, **2**, 1950–1952.

11 Q. Chen, J. X. Wang, Q. Wang, N. Bian, Z. H. Li, C. G. Yan and B. H. Han, *Macromolecules*, 2011, **44**, 7987–7993.

12 Q. Chen, J. X. Wang, F. Yang, D. Zhou, N. Bian, X. J. Zhang, C. G. Yan and B. H. Han, *J. Mater. Chem.*, 2011, **21**, 13554–13560.

13 C. G. Bezzu, M. Carta, A. Tonkins, J. C. Jansen, P. Bernardo, F. Bazzarelli and N. B. McKeown, *Adv. Mater.*, 2012, **24**, 5930–5933.

14 X. M. Guan, C. D. Zhao, X. Y. Liu and H. X. Zhang, *J. Chromatogr. A*, 2013, **1302**, 28–33.

15 X. H. Ma, O. Salinas, E. Litwiller and I. Pinnau, *Macromolecules*, 2013, **46**, 9618–9624.

16 X. H. Ma, O. Salinas, E. Litwiller and I. Pinnau, *Polym. Chem.*, 2014, **5**, 6914–6922.

17 L. J. Feng, J. W. Guo, X. Zhong and Z. Y. Sun, *J. Macromol. Sci., Part A: Pure Appl. Chem.*, 2014, **51**, 604–609.

18 X. H. Ma, B. Ghanem, O. Salines, E. Litwiller and I. Pinnau, *ACS Macro Lett.*, 2015, **4**, 231–235.

19 Z. L. Wu, B. C. Han, C. H. Zhang, D. Y. Zhu, B. Peng, L. X. Gao, M. X. Ding and Z. H. Yang, *High Perform. Polym.*, 2015, **27**, 288–298.

20 R. G. D. Taylor, C. G. Bezzu, M. Carta, K. J. Msayib, J. Walker, R. Short, B. M. Kariuki and N. B. McKeown, *Chem. – Eur. J.*, 2016, **22**, 2466–2472.

21 I. Pyka, D. Lubczyk, M. D. S. Saiju, J. Salbeck and S. R. Waldvogel, *ChemPlusChem*, 2017, **82**, 1116–1120.

22 I. Pyka, J. Nikl, D. Schollmeyer and S. R. Waldvogel, *Eur. J. Org. Chem.*, 2017, 3501–3504.

23 C. G. Bezzu, M. Carta, M. C. Ferrari, J. C. Jansen, M. Monteleone, E. Esposito, A. Fuoco, K. Hart, T. P. Liyana-Arachchi, C. M. Colina and N. B. McKeown, *J. Mater. Chem. A*, 2018, **6**, 10507–10514.

24 J. Schmidt, M. Werner and A. Thomas, *Macromolecules*, 2009, **42**, 4426–4429.

25 B. G. Hauser, O. K. Farha, J. Exley and J. T. Hupp, *Chem. Mater.*, 2013, **25**, 12–16.

26 L. Pop, F. Dumitru, N. D. Hadade, Y. M. Legrand, A. van der Lee, M. Barboiu and I. Grosu, *Org. Lett.*, 2015, **17**, 3494–3497.

27 L. Pop, M. L. Golban, N. D. Hadade, C. Socaci and I. Grosu, *Synthesis*, 2015, 2799–2804.

28 M. M. Trandafir, L. Pop, N. D. Hadade, I. Hristea, C. M. Teodorescu, F. Krumeich, J. A. van Bokhoven, I. Grosu and V. I. Parvulescu, *ChemCatChem*, 2019, **11**, 538–549.

29 (*a*) H. Gilman and R. D. Gorsich, *J. Am. Chem. Soc.*, 1958, **80**, 1883–1886; (*b*) Q. Hou, N. Y. Li, Y. Zhang, J. G. Liu and H. Zhu, *Adv. Mater. Res.*, 2011, **415-417**, 1364–1367.

30 S. H. Lee, B. B. Jang and Z. H. Kafafi, *J. Am. Chem. Soc.*, 2005, **127**, 9071–9078.

31 J. J. McDowell, D. Gao, D. S. Seferos and G. Ozin, *Polym. Chem.*, 2015, **6**, 3781–3789.

32 Y. Nishii, M. Ikeda, Y. Hayashi, S. Kawauchi and M. Miura, *J. Am. Chem. Soc.*, 2020, **142**, 1621–1629.

33 H. B. Xiao, B. Leng and H. Tian, *Polymer*, 2005, **46**, 5707–5713.

34 X. S. Xu, X. F. Li, S. M. Wang, J. Q. Ding and L. X. Wang, *J. Mater. Chem. C*, 2018, **6**, 9599–9606.

35 G. C. Yang, Z. M. Su and C. S. Qin, *J. Phys. Chem. A*, 2006, **110**, 4817–4821.

36 S. Yamaguchi and K. Tamao, *Bull. Chem. Soc. Jpn.*, 1996, **69**, 2327–2334.

37 M. Thommes, K. Kaneko, A. V. Neimark, J. P. Olivier, F. Rodriguez-Reinoso, J. Rouquerol and K. S. W. Sing, *Pure Appl. Chem.*, 2015, **87**, 1051–1069.

38 J. C. Sanchez, A. G. DiPasquale, A. L. Rheingold and W. C. Trogler, *Chem. Mater.*, 2007, **19**, 6459–6470.

39 J. C. Sanchez and W. C. Trogler, *J. Mater. Chem.*, 2008, **18**, 3143–3156.

40 J. C. Sanchez, S. A. Urbas, S. J. Toal, A. G. DiPasquale, A. L. Rheingold and W. C. Trogler, *Macromolecules*, 2008, **41**, 1237–1245.

41 J. A. Yang, S. Aschemeyer, H. P. Martinez and W. C. Trogler, *Chem. Commun.*, 2010, **46**, 6804–6806.

42 B. Dedeoglu, V. Ayiyente and A. S. Ozen, *J. Phys. Chem. C*, 2014, **118**, 6385–6397.

43 B. Dedeoglu, A. Monari, T. Etienne, V. Aviyente and A. S. Ozen, *J. Phys. Chem. C*, 2014, **118**, 23946–23953.

44 K. L. Chan, S. E. Watkins, C. S. K. Mak, M. J. McKiernan, C. R. Towns, S. I. Pascu and A. B. Holmes, *Chem. Commun.*, 2005, 5766–5768.

45 C. W. Keyworth, K. L. Chan, J. G. Labram, T. D. Anthopoulos, S. E. Watkins, M. McKiernan, A. J. P. White, A. B. Holmes and C. K. Williams, *J. Mater. Chem.*, 2011, **21**, 11800–11814.